# Dosimetric results in treatments of neuroblastoma and neuroendocrine tumors with (131)I-metaiodobenzylguanidine with implications for the activity to administer.

MINGUEZ GABINA, PABLO; Flux, Glenn; Genolla, Jose; Guayambuco, Sonia; Delgado, Alejandro; Fombellida, Jose Cruz; Sjögreen Gleisner, Katarina

*Published in:*
Medical Physics

*DOI:*
10.1118/1.4921807

2015

*Document Version:*
Peer reviewed version (aka post-print)

# Dosimetric results in treatments of neuroblastoma and neuroendocrine tumors with $^{131}$I-metaiodobenzylguanidine with implications for the activity to administer

**Pablo Mínguez**[a)]
Department of Medical Radiation Physics, Lund University, Lund, Sweden
Department of Medical Physics, Gurutzeta/Cruces University Hospital, Barakaldo, Spain

**Glenn Flux**
Joint Department of Physics, Royal Marsden NHS Foundation Trust & Institute of Cancer Research, Sutton, UK

**José Genollá**
Department of Nuclear Medicine, Gurutzeta/Cruces University Hospital, Barakaldo, Spain

**Sonía Guayambuco**
Department of Nuclear Medicine, Gurutzeta/Cruces University Hospital, Barakaldo, Spain

**Alejandro Delgado**
Department of Nuclear Medicine, Gurutzeta/Cruces University Hospital, Barakaldo, Spain

**José Cruz Fombellida**
Department of Nuclear Medicine, Gurutzeta/Cruces University Hospital, Barakaldo, Spain

**Katarina Sjögreen Gleisner**
Department of Medical Radiation Physics, Lund University, Lund, Sweden

**Purpose:** The aim was to investigate whole-body and red-marrow absorbed doses in treatments of neuroblastoma (NB) and adult neuroendocrine tumors (NET) with $^{131}$I-metaiodobenzylguanidine (mIBG), and to propose a simple method for determining the activity to administer when dosimetric data for the individual patient are not available.

**Methods:** Nine NB patients and six NET patients were included, giving in total 19 treatments as four patients were treated twice. Whole-body absorbed doses were determined from dose-rate measurements and planar gamma-camera imaging. For six NB and five NET treatments, red-marrow absorbed doses were also determined using the blood-based method.

**Results:** Dosimetric data from repeated administrations in the same patient were consistent. In groups of NB and NET patients, similar whole-body residence times were obtained, implying that whole-body absorbed dose per unit of administered activity could be reasonably well described as a power function of the patient mass. For NB, this functional form was found to be consistent with dosimetric data from previously published studies. The whole-

body to red-marrow absorbed dose ratio was similar among patients, with values of 1.4±0.6 to 1.7±0.7 (1 standard deviation) in NB treatments, and between 1.5±0.6 and 1.7±0.7 (1 standard deviation) in NET treatments.

**Conclusions:** The consistency of dosimetric results between administrations for the same patient supports prescription of the activity based on dosimetry performed in pre-treatment studies, or during the first administration in a fractionated schedule. The expressions obtained for whole-body absorbed doses per unit of administered activity as a function of patient mass for NB and NET treatments are believed to be a useful tool to estimate the activity to administer at the stage when the individual patient biokinetics has not yet been measured.

Key words: Neuroblastoma, Neuroendocrine tumors, Treatment schedule, $^{131}$I-mIBG.

## 1. INTRODUCTION

In treatments of neuroblastoma (NB) and adult neuroendocrine tumors (NET), surgery is the first-line therapy with the aim of achieving a complete cure[1,2]. If radical surgery is not feasible, multimodal treatment options include surgery, chemotherapy, external beam radiotherapy (EBRT) and molecular radiotherapy (MRT)[3]. $^{131}$I-mIBG therapy is administered for inoperable pheocromocytomas, paragangliomas, carcinoid tumors, stage III or IV relapsed or primary refractory NBs and metastatic or recurrent medullary thyroid cancers[4]. The number of patients treated with $^{131}$I-mIBG is usually limited compared to the total number of NB and NET patients as $^{131}$I-mIBG therapy is frequently considered only when other treatment modalities have been exhausted.

During the last two decades several studies have been published on the use of $^{131}$I-mIBG for NB and NET treatments[5-12], and guidelines have been provided by the European Association of Nuclear Medicine (EANM)[4]. The administered activity is most commonly prescribed using

fixed activities[13,14] or a specified activity per patient mass[15-18] or per body surface[19]. Some studies have shown an improved treatment outcome with increased administered activities[20,21]. In NB treatments, the most established schedule is given by Gaze *et al.*[17]. In this protocol, two treatment administrations separated by a fortnight are given where the first is prescribed as activity per body mass (444 MBq/kg), and the second is tailored to deliver a whole-body absorbed dose of 4 Gy in total for the two administrations. In NET treatments, where dosimetric data are still limited[22], established schedules are currently lacking, although in principle a similar dosimetry-based approach could be adopted. In both NB and NET treatments, there is a need to compile experience and working knowledge of clinically obtained whole-body absorbed doses per unit of administered activity. Such information can be used to improve estimates of the activity to administer at the stage when dosimetric data are lacking, such as for the first activity administration in a fractionated schedule.

Hematologic toxicity is dose limiting in $^{131}$I-mIBG therapy[23-25]. When activities above 444 MBq/kg are administered, harvesting of autologous tumor-free, hematopoietic stem cells must be performed before treatment[26]. In the schedule by Gaze *et al.*[17], stem-cell rescue is performed after approximately four weeks from the first administration, when the activity in the body has decreased below 30 MBq. When stem cells are not available, it must be ensured that the administered activity does not exceed levels that may induce non-tolerable red-marrow absorbed doses. Here, the use of whole-body dosimetry as a surrogate for red-marrow dosimetry has been established[27]. This obviates the need for repeated blood sampling, which is considered invasive, particularly in children. However, as pointed out in a recent review[12], no study has yet focused on the difference between whole-body and red-marrow absorbed doses.

This study reports on dosimetric results from $^{131}$I-mIBG NB and NET treatments in the Gurutzeta-Cruces University Hospital during the last six years. The aim is to investigate

absorbed doses for whole body and red marrow. A further aim is to propose a simple method for determining the activity to administer at the stage when dosimetric data are not available for the individual patient, based on data acquired in this study and in the context of other published studies. The recommendations of the EANM[28] have been taken into account in the composition of the paper.

## 2. METHODS

### 2.A. Patient population and administrations

#### NB treatments

Nine patients (six male and three female, age 3y−22y) with relapsed stage-4 NB were included. Three patients were given two treatments separated by more than one year, with the result that twelve treatments were considered in total. Further on, NB treatments are denoted $T_{NB}1$—$T_{NB}9$, with postscripts *a* and *b* to indicate repeated treatment of the same patient. A summary of treatment data including patient mass, $m_p$, administered activity, $A_{adm}$, and performed measurements is given in Table 1. Treatments $T_{NB}1a$, $T_{NB}2$, $T_{NB}3$, $T_{NB}4$, $T_{NB}6a$, $T_{NB}7$ and $T_{NB}8$ were performed following the schedule by Gaze *et al.*[17]. Treatments $T_{NB}1b$, $T_{NB}5$, $T_{NB}6b$, $T_{NB}4$ and $T_{NB}9b$ were performed without concomitant chemotherapy and stem cell support in one or two fractions (see Table 1) aiming at giving a whole-body absorbed dose, $D_{wb}$, of 2 Gy. Treatment $T_{NB}9a$ was performed with concomitant chemotherapy and stem cell support but did not follow the schedule by Gaze *et al.*[17] to avoid exceeding $A_{adm}$ of 37 GBq. The timing of stem cell support was approximately 4 weeks post-$^{131}$I-mIBG administration, as determined using dose-rate measurements.

| Treatment | $m_p$ (kg) | $A_{adm}$ (GBq) | | | Performed measurements | |
|---|---|---|---|---|---|---|
| | | Adm 1 | Adm 2 | Total | Adm 1 | Adm 2 |
| $T_{NB}1a$ | 11 | 5.0 | 5.5 | 10.5 | DR/BD | DR |
| $T_{NB}1b$ (+13 months)* | 13 | 5.5 | N/A | 5.5 | DR | *N/A* |
| $T_{NB}2$ | 13 | 5.7 | 13.7 | 19.4 | DR/BD | DR |
| $T_{NB}3$ | 14 | 6.3 | 6.7 | 13.0 | DR/BD/PL | DR/BD/PL |
| $T_{NB}4$ | 17 | 7.7 | 6.5 | 14.2 | DR | DR |
| $T_{NB}5$ | 18 | 4.2 | 3.7 | 7.9 | DR | DR |
| $T_{NB}6a$ | 20 | 9.0 | 8.3 | 17.3 | DR/BD | DR |
| $T_{NB}6b$ (+35 months)* | 24 | 10.8 | N/A | 10.8 | DR | *N/A* |
| $T_{NB}7$ | 22 | 9.8 | 9.8 | 19.6 | DR | DR |
| $T_{NB}8$ | 32 | 13.0 | 14.4 | 27.4 | DR | DR |
| $T_{NB}9a$ | 63 | 11.1 | 22.2 | 33.3 | DR/BD | DR |
| $T_{NB}9b$ (+16 months)* | 63 | 10.5 | 10.4 | 20.9 | DR/BD/PL | DR/BD/PL |

Table 1. Data of NB treatments. DR=Dose-rate measurement. BD=Blood dosimetry. PL=Planar imaging. Adm=Administration. *Time between repeated treatments.

## NET treatments

Six NET patients were included (five female and one male, age 21y−80y). One patient was treated twice, so in total seven treatments were considered. Further on, NET treatments are denoted $T_{NET}1$—$T_{NET}6$, with postscripts *a* and *b* to indicate repeated treatment. A summary of treatment data is given in Table 2. For $T_{NET}2$, $T_{NET}3$, $T_{NET}5$, $T_{NET}6a$ and $T_{NET}6b$, a pre-treatment dosimetry study was also performed approximately one month before treatment.

| Treatment | $m_p$ (kg) | $A_{adm}$ (GBq) | | | | Performed measurements | | |
|---|---|---|---|---|---|---|---|---|
| | | Pre-Tr Adm | Adm 1 | Adm 2 | Total (Adm 1 + Adm 2) | Pre-Tr Adm | Adm 1 | Adm 2 |
| $T_{NET}1$ (paraganglioma) | 58 | N/A | 16.2 | N/A | 16.2 | N/A | DR | N/A |
| $T_{NET}2$ (carcinoid tumor) | 44 | 0.44 | 21.2 | N/A | 21.2 | PL/BD | DR | N/A |
| $T_{NET}3$ (pheochromocytoma) | 66 | 0.071 | 14.4 | N/A | 14.4 | PL/BD | DR | N/A |
| $T_{NET}4$ (pheochromocytoma) | 49 | N/A | 5.6 | 7.8 | 13.4 | N/A | DR | DR |
| $T_{NET}5$ (carcinoid tumor) | 80 | 0.23 | 9.0 | 8.6 | 17.6 | PL/BD | DR/BD | DR |
| $T_{NET}6a$ (pheochromocytoma ) | 49 | 0.19 | 7.8 | N/A | 7.8 | PL/BD | DR | N/A |
| $T_{NET}6b$ (pheochromocytoma) (+1 year)* | 49 | 0.20 | 8.4 | 9.6 | 18.0 | PL/BD | DR | DR |

Table 2. Data of NET treatments, including diagnosis. DR=Dose-rate measurement. BD=Blood dosimetry. PL=Planar imaging. Pre-Tr Adm=Pre-treatment administration. Adm=Administration. *Time between repeated treatments.

Specific activity of the administered $^{131}$I-mIBG was 1110 MBq/mg. In both NB and NET treatments, the average time as inpatients was five days in each administration (range four−six days) and patients were released according to Spanish national regulations, in agreement with recommendations of the IAEA[29]. The therapeutic use of $^{131}$I-mIBG is approved by the Spanish Agency of Medicines and Medical Devices and informed consent from all patients, or from their parents in the case of children, was obtained.

**2.B. Data acquisition and activity quantification**

Dose-rate measurements were performed during the time as inpatients for estimation of the whole-body time-activity curve (see Tables 1 and 2). Measurements were performed using a handheld, pressurized ion-chamber survey-meter, Inovision Model 451P, Fluke Biomedical (Eindhoven, The Netherlands). Acquisitions were made at distances of 1 m and 2 m from standing patients at marked positions on the floor, in both anterior and posterior directions. The height of the detector in relation to the floor was held constant with reference to an external mark, and all measurements were made by trained staff. The first measurement was performed immediately after the administration to obtain a reading corresponding to the total $A_{adm}$. Remaining measurements were made approximately every two hours during the first day, every four hours during the second day and every six hours during the remaining days, aiming at performing acquisitions after bladder voids. In total this yielded approximately 20 time points for each treatment. The signal-to-noise ratio, estimated by dividing the patient readings with the variability in background readings, was above 20 in all measurements, and dead-time effects were negligible. A sequence of whole-body time-activity values, $A_{wb}(t)$, was determined from the anterior and posterior readings, $R_A(t)$ and $R_P(t)$, for each patient-detector distance according to

$$A_{wb}(t) = A_{adm}\frac{\sqrt{R_A(t)R_P(t)}}{\sqrt{R_A(0)R_P(0)}} = A_{adm}\, r(t) \quad (1)$$

where $r(t)$ were the relative values obtained from measurement, with $r(0)$ =1. The $A_{wb}(t)$ values from measurements at 1 m and 2 m differed less than 5%, and the average value was therefore used. A dose calibrator, Capintec CRC®-15R, (Capintec, Inc Ramsey, NJ, USA), was used for measurements of $A_{adm}$.

Planar imaging using a gamma camera was employed to estimate the whole-body time-activity curve in NET pre-treatment dosimetric studies, and also in two NB treatments for comparison to dose-rate meter derived values (Tables 1 and 2). Acquisitions were made employing a dual-head General Electric (GE, Fairfield, CT, USA) Infinia Hawkeye gamma camera, with a crystal thickness of 9.5 mm and equipped with High-Energy General-Purpose collimators. A scan speed of 12 cm/min, a matrix size of 256×1024, and an energy window of 20% centered at 364 keV were used. For the NET pre-treatment dosimetric studies, in which acquisitions were performed a few minutes, 24 h, 48 h and 120 h after the administration, the administered activity was low and dead-time effects were thus negligible. To avoid dead-time effects for NB patients, where pre-treatment imaging was not performed, the first therapy administration was separated into two fractions. Approximately 370 MBq was injected and a whole-body scan was performed. Immediately after this acquisition, the rest of the activity was injected. The remaining acquisitions were performed approximately at 48 h and 115 h. In all the acquisitions performed, the count rate was below 10000 counts per second. The whole-body activity was determined using Eq. (1), where $R_A(t)$ and $R_P(t)$ were then the net count rates in regions of interest (ROIs) encompassing the body in anterior and posterior images, subtracted by the count rate in background ROIs rescaled to the area of the whole-body ROI, to partly compensate for septal penetration and scatter.

Blood sampling was performed in six NB treatments, five NET pre-treatment studies, and one NET treatment, for the purpose of red-marrow dosimetry (see Tables 1 and 2). For NB patients blood sampling was performed at a few minutes, 6 h, 24 h, 48 h, 72 h, and 96 h or

115 h after injection, whereas for NET patients, blood sampling was made at a few minutes, 6 h, 24 h, 48 h, and 120 h. Blood samples of 1 ml or 2 ml volume were prepared using a pipette, and were then allowed to decay to avoid dead-time effects. Measurements were performed using a calibrated γ-well counter 1282 Compugamma CS LKB Wallac (Melbourne, Australia). The activity concentration was determined by dividing the obtained count rate by a pre-determined calibration factor and the sample volume.

**2.C. Dosimetric calculations**

$D_{wb}$ were calculated following the standard MIRD methodology[30], as described in Appendix A. Blood-based calculation of red-marrow absorbed dose, $D_{rm}$, was carried out according to procedures in the EANM guidelines[26] and to the MIRD formalism, including source terms from activity in the red marrow and in the remainder of the body for the self- and cross-absorbed dose, respectively, as described in Appendix B. Additionally, the method described by Traino *et al.*[31] was used.

The standard deviations in $D_{wb}$ and $D_{rm}$ were estimated by uncertainty propagation[32], as described in Appendix C. For both $D_{wb}$ and the whole-body residence time, $\tau_{wb}$, the relative standard deviation was estimated to be 20%. The main contribution to $D_{rm}$ was the cross-absorbed dose from the remainder of the body, and the relative standard deviation for $D_{rm}$ was thus also estimated to be 20%. These uncertainties are in line with values suggested by others[33,34].

**2.D. Hematologic toxicities**

The post-therapy platelet, neutrophil and leukocyte nadir was obtained in NET treatments in order to study hematologic toxicity. The grade of toxicity was analyzed according to the Common Terminology Criteria of Adverse Events (CTCAE), version 3[35] (available at http://ctep.cancer.gov/protocolDevelopment/electronic_applications/docs/ctcaev3.pdf). In

NB treatments the grade of hematologic toxicity was not quantified, since in the majority of treatments the intent was aplasia.

## 3. RESULTS

### 3.A. NB treatments

Table 3 summarizes values obtained for $\tau_{wb}$ and $D_{wb}/A_{adm}$. The mean value of $D_{wb}/A_{adm}$ was 0.22 ±0.04 (1 standard deviation) Gy/GBq (median 0.22 Gy/GBq). For all treatments except $T_{NB}2$, where the patient suffered from nephropathy and thus had a shorter $\tau_{wb}$, values of $\tau_{wb}$ were within 25.1 h - 29.3 h (mean 27.1 ±5.4 h, median 26.7 h). For the patients that followed the schedule by Gaze *et al.*[17], that is, those who were prescribed a $D_{wb}$ of 4 Gy in two administrations, the prescription was followed to within 0.1 Gy.

| Treatment | $\tau_{wb}$ (h) | | $D_{wb}/A_{adm}$ (Gy/GBq) | | | $D_{wb}$ (Gy) | | |
|---|---|---|---|---|---|---|---|---|
| | Adm 1 | Adm 2 | Adm 1 | Adm 2 | Total | Adm 1 | Adm 2 | Total |
| $T_{NB}1a$ | 26.5±5.3 | 25.5±5.1 | 0.38±0.08 | 0.36±0.07 | 0.37±0.07 | 1.9±0.4 | 2.0±0.4 | 3.9±0.8 |
| $T_{NB}1b$ | 25.1±5.0 | N/A | 0.33±0.07 | N/A | 0.33±0.07 | 1.8±0.4 | N/A | 1.8±0.4 |
| $T_{NB}2$ | 15.9±3.2 | 16.0±3.2 | 0.21±0.04 | 0.20±0.04 | 0.21±0.04 | 1.2±0.2 | 2.8±0.6 | 4.0±0.8 |
| $T_{NB}3$ | 26.7±5.3 | 28.2±5.6 | 0.30±0.06 | 0.33±0.07 | 0.32±0.06 | 1.9±0.4 | 2.2±0.4 | 4.1±0.8 |
| $T_{NB}4$ | 28.6±5.7 | 28.3±5.7 | 0.29±0.06 | 0.28±0.06 | 0.28±0.06 | 2.2±0.4 | 1.8±0.4 | 4.0±0.8 |
| $T_{NB}5$ | 25.5±5.1 | 25.2±5.0 | 0.24±0.05 | 0.22±0.04 | 0.23±0.05 | 1.0±0.2 | 0.8±0.2 | 1.8±0.4 |
| $T_{NB}6a$ | 27.3±5.5 | 27.9±5.6 | 0.23±0.05 | 0.24±0.05 | 0.24±0.05 | 2.1±0.4 | 2.0±0.4 | 4.1±0.8 |
| $T_{NB}6b$ | 26.3±5.3 | N/A | 0.19±0.04 | N/A | 0.19±0.04 | 2.0±0.4 | N/A | 2.0±0.4 |
| $T_{NB}7$ | 26.0±5.2 | 26.2±5.2 | 0.19±0.04 | 0.20±0.04 | 0.20±0.04 | 1.9±0.4 | 2.0±0.4 | 3.9±0.8 |
| $T_{NB}8$ | 26.6±5.3 | 26.1±5.2 | 0.15±0.03 | 0.15±0.03 | 0.15±0.03 | 1.9±0.4 | 2.1±0.4 | 4.0±0.8 |
| $T_{NB}9a$ | 29.3±5.9 | 28.9±5.8 | 0.09±0.02 | 0.09±0.02 | 0.09±0.02 | 1.0±0.2 | 1.9±0.4 | 2.9±0.6 |
| $T_{NB}9b$ | 28.8±5.8 | 28.9±5.8 | 0.09±0.02 | 0.09±0.02 | 0.09±0.02 | 0.9±0.2 | 0.9±0.2 | 1.8±0.4 |

Table 3. Results for $\tau_{wb}$, $D_{wb}/A_{adm}$ and $D_{wb}$ in NB treatments

Data in Table 3 are based on probe-based dose-rate measurements. Figure 1 shows a comparison between $A_{wb}$ ($t$) derived from dose-rate measurements and gamma camera images for $T_{NB}3$. Differences between values obtained from imaging and dose-rate measurements were within 10% for both $T_{NB}3$ and $T_{NB}9b$.

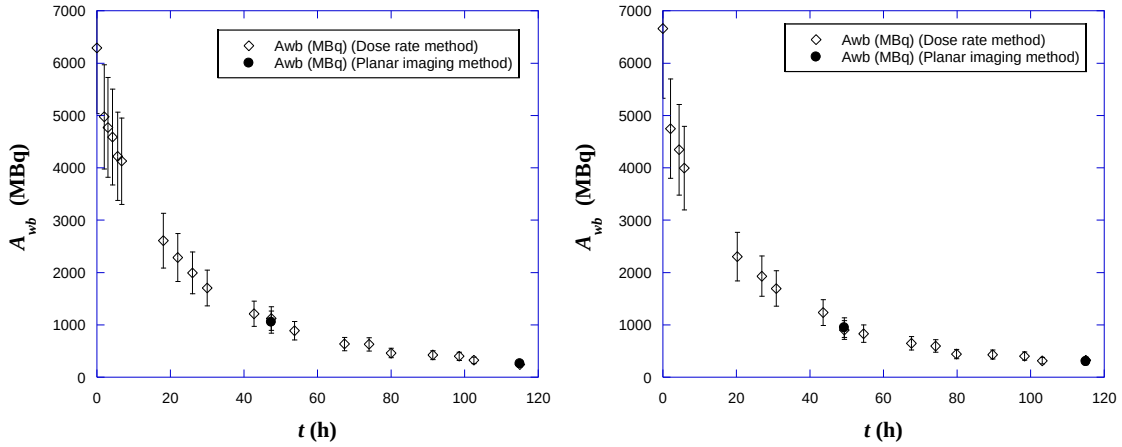


Figure 1. Results for $A_{wb}(t)$, for the first (left panel), and second administration (right panel), in $T_{NB}3$. Open symbols are from dose-rate measurements, and closed symbols are from whole-body planar images acquired at 48h and 115h.

Table 4 shows the results of $D_{rm}$ and $D_{rm}/A_{adm}$. For $T_{NB}1b$, $T_{NB}4$, $T_{NB}5$, $T_{NB}6b$, $T_{NB}7$ and $T_{NB}8$ red-marrow dosimetry could not be performed due to lack of blood samples. Following the procedure by Traino *et al.*[31] values obtained for $D_{rm}$ were lower, but within 10 % of values of $D_{rm}$ in Table 4. The self-absorbed dose was between 9% and 11% of the total $D_{rm}$. For the two treatments where measurements were made in both administrations ($T_{NB}3$ and $T_{NB}9b$), the ratio $D_{rm}/A_{adm}$ was approximately equal. For the other treatments, $D_{rm}$ for the second administration was thus estimated by assuming an equal $D_{rm}/A_{adm}$ between administrations. Table 4 also shows the ratio $D_{wb}/D_{rm}$, which ranged from 1.4 to 1.7 (mean 1.5±0.6, median 1.5).

| Treatment | Adm 1 | | Adm 2 | | Both Adm | |
|---|---|---|---|---|---|---|
| | $D_{rm}$ (Gy) | $D_{rm}/A_{adm}$ (Gy/GBq) | $D_{rm}$ (Gy) | $D_{rm}/A_{adm}$ (Gy/GBq) | $D_{rm}$ (Gy) | $D_{wb}/D_{rm}$ |
| $T_{NB}1a$ | 1.4±0.3 | 0.27±0.05 | 1.5±0.3* | N/A | 2.9±0.6 | 1.4±0.6 |
| $T_{NB}2$ | 0.8±0.2 | 0.15±0.03 | 2.0±0.4* | N/A | 2.9±0.6 | 1.4±0.6 |
| $T_{NB}3$ | 1.1±0.2 | 0.18±0.04 | 1.3±0.3 | 0.19±0.04 | 2.4±0.5 | 1.7±0.7 |
| $T_{NB}6a$ | 1.0±0.3 | 0.14±0.03 | 1.2±0.2* | N/A | 2.5±0.5 | 1.6±0.6 |
| $T_{NB}9a$ | 0.6±0.1 | 0.06±0.01 | 1.3±0.3* | N/A | 1.9±0.4 | 1.5±0.6 |
| $T_{NB}9b$ | 0.6±0.1 | 0.05±0.01 | 0.6±0.1 | 0.06±0.01 | 1.2±0.2 | 1.5±0.6 |

Table 4. Results for $D_{rm}$ and $D_{rm}/A_{adm}$, in administrations 1 and 2, in NB treatments. For both administrations, the values of the total $D_{rm}$ and $D_{wb}/D_{rm}$ are shown. * Extrapolated values obtained by assuming the value of $D_{rm}/A_{adm}$ obtained for the first administration.

### 3.B. NET treatments

Table 5 summarizes the values obtained for $\tau_{wb}$ and $D_{wb}/A_{adm}$. The mean value of $D_{wb}/A_{adm}$ was 0.16±0.03 Gy/GBq (median 0.13 Gy/GBq). With the exception of $T_{NET}4$ and $T_{NET}5$, who suffered from a large tumor burden and thus had notably longer $\tau_{wb}$, values of $\tau_{wb}$ were within the range 31.0 h — 35.2 h (mean 33.1 ±6.6 h, median 33.3 h).

| Treatment | $\tau_{wb}$ (h) | | $D_{wb}/A_{adm}$ (Gy/GBq) | | | $D_{wb}$ (Gy) | | |
|---|---|---|---|---|---|---|---|---|
| | Adm 1 | Adm 2 | Adm 1 | Adm 2 | Total | Adm 1 | Adm 2 | Total |
| $T_{NET}1$ | 32.1±6.4 | N/A | 0.10±0.02 | N/A | 0.10±0.02 | 1.7±0.3 | N/A | 1.7±0.3 |
| $T_{NET}2$ | 35.2±7.0 | N/A | 0.15±0.03 | N/A | 0.15±0.03 | 3.1±0.6 | N/A | 3.1±0.6 |
| $T_{NET}3$ | 31.0±6.2 | N/A | 0.09±0.02 | N/A | 0.09±0.02 | 1.3±0.3 | N/A | 1.3±0.3 |
| $T_{NET}4$ | 82.2±16.4 | 82.6±16.5 | 0.30±0.06 | 0.31±0.06 | 0.31±0.06 | 1.7±0.3 | 2.4±0.5 | 4.1±0.8 |
| $T_{NET}5$ | 69.5±13.9 | 58.2±11.6 | 0.17±0.03 | 0.14±0.03 | 0.15±0.03 | 1.5±0.3 | 1.2±0.2 | 2.7±0.5 |
| $T_{NET}6a$ | 33.1±6.6 | N/A | 0.13±0.03 | N/A | 0.13±0.03 | 1.0±0.2 | N/A | 1.0±0.2 |
| $T_{NET}6b$ | 33.7±6.7 | 33.5±6.7 | 0.13±0.03 | 0.14±0.03 | 0.13±0.03 | 1.1±0.2 | 1.3±0.3 | 2.4±0.5 |

Table 5. Results for $\tau_{wb}$, $D_{wb}/A_{adm}$ and $D_{wb}$ in NET treatments.

Table 6 shows $D_{rm}/A_{adm}$ obtained for pre-treatment dosimetric studies. In $T_{NET}1$ and $T_{NET}4$ blood samples could not be obtained. Following the procedure by Traino *et al.*[31] lower values for $D_{rm}$ were obtained, but within 10% of values of $D_{rm}$ in Table 6. The self-absorbed dose was between 14% and 18% of the total $D_{rm}$. For $T_{NET}5$, $D_{rm}$ was also calculated during the first treatment administration. The value of $D_{rm}/A_{adm}$ obtained was 0.10±0.02 Gy/GBq, which was thus in agreement with that of the pre-treatment study. Table 6 also shows the ratio $D_{wb}/D_{rm}$, which ranged between 1.5 and 1.7 (mean 1.6±0.6, median 1.7).

| Pre-treatment study | $D_{rm}/A_{adm}$ (Gy/GBq) | $D_{wb}/D_{rm}$ |
|---|---|---|
| $T_{NET}2$ | 0.08±0.02 | 1.7±0.7 |
| $T_{NET}3$ | 0.06±0.01 | 1.5±0.6 |
| $T_{NET}5$ | 0.09±0.02 | 1.7±0.7 |
| $T_{NET}6a$ | 0.07±0.01 | 1.7±0.7 |
| $T_{NET}6b$ | 0.08±0.02 | 1.6±0.6 |

Table 6. Results for $D_{rm}/A_{adm,}$ and $D_{wb}/D_{rm}$ in pre-treatment dosimetric studies in NET patients.

The grade of toxicity in NET treatments is shown in Table 7. No correlation between the grade of toxicity in platelets, leukocytes and neutrophils and $D_{wb}$ or $D_{rm}$ was found. However, there was a tendency that toxicity was more pronounced for elderly patients than for younger ones.

| Treatment | Grade of toxicity | | | Patients' age (y) |
|---|---|---|---|---|
| | Platelets | Leukocytes | Neutrophils | |
| $T_{NET}1$ | None | None | None | 24 |
| $T_{NET}2$ | 3 | 4 | 4 | 73 |
| $T_{NET}3$ | 4 | 4 | 4 | 62 |
| $T_{NET}4$ | 3 | 3 | 2 | 60 |
| $T_{NET}5$ | 3 | 3 | 2 | 80 |
| $T_{NET}6a$ | None | None | None | 27 |
| $T_{NET}6b$ | None | None | None | 28 |

Table 7. Grade of toxicity in NET treatments.

### 3.C. Analysis of dosimetric results for NBs and NETs

Figure 2 shows the ratio $D_{wb}/A_{adm}$ for both NB and NET treatments, and a large variability between patients can be observed. Values of $D_{wb}/A_{adm}$ for repeated administrations (including treatments and pre-treatment dosimetric studies) in the same patient were consistent, thus supporting the concept of performing absorbed dose planning for subsequent administrations.

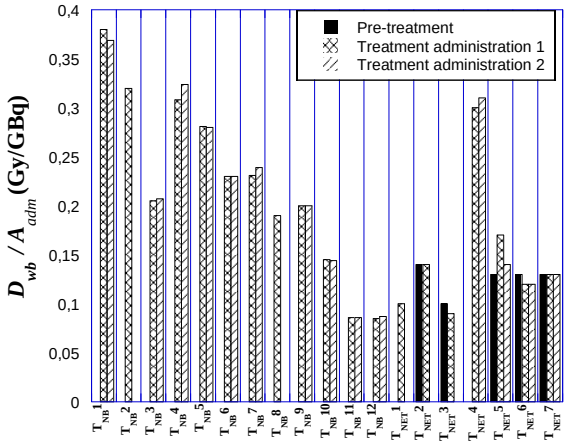


Figure 2. Results obtained for $D_{wb}/A_{adm}$ in NB treatments and in NET pre-treatment and treatment studies.

As seen in Table 3, a similar $\tau_{wb}$ was obtained in NB treatments, except for $T_{NB}2$. If inserting one single value of $\tau_{wb}$ into Eq. (A1), the ratio $D_{wb}/A_{adm}$ follows a power dependence with $m_p$. Using the mean value of $\tau_{wb}$ obtained in this study, the following Equation was obtained:

$$(D_{wb}/A_{adm})_{NB} = 3.63\ m_p{}^{-0.921} \qquad (2)$$

in unit of Gy/GBq. Results of Eq. (2) were compared to results from previously published studies, using data of $D_{wb}/A_{adm}$ for NB treatments as retrieved from the study by Toporski *et al.*[11] performed at Lund University Hospital, Sweden, and from the study by Buckley *et al.*[25] performed at Royal Marsden Hospital, UK. To rule out inconsistencies in calculation methods among centers, a small comparison exercise was undertaken sharing three sets of acquired time-dose rate data. $D_{wb}$ were calculated at each of the three centers, with results obtained of within ±10% from the mean value, thus supporting a combined data analysis. Figure 3 shows Eq. (2) in relation to data acquired in this study, and combined with data from Toporski *et al.*[11] and Buckley *et al.*[25].

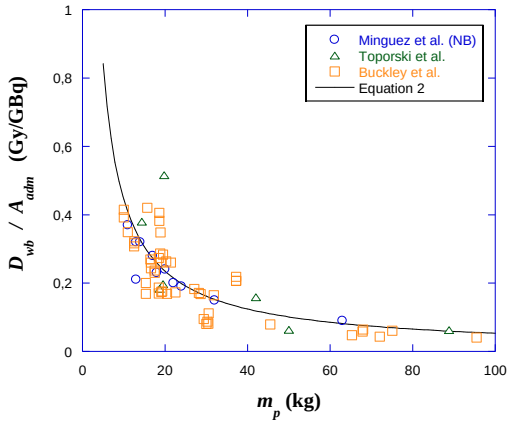


Figure 3. Results for $D_{wb}/A_{adm}$ as function of $m_p$ from Toporski *et al.*[11], Buckley *et al.*[25], and data obtained in this study. The solid line shows the curve obtained from Eq. (2).

Regarding NET (Table 5), similar values of $\tau_{wb}$ were obtained for the five treatments with modest tumor burden. Inserting the mean value obtained into Eq. (A1), the following Equation was obtained:

$$(D_{wb}/A_{adm})_{NET} = 4.44\ m_p^{-0.921} \quad (3)$$

Figure 4 shows $D_{wb}/A_{adm}$ as a function of $m_p$ using Eq. (3). Comparing the graphs for NB and NET treatments (Figure 4, right panel), differences in $D_{wb}/A_{adm}$ values were small for adult masses but increased slightly for pediatric masses.

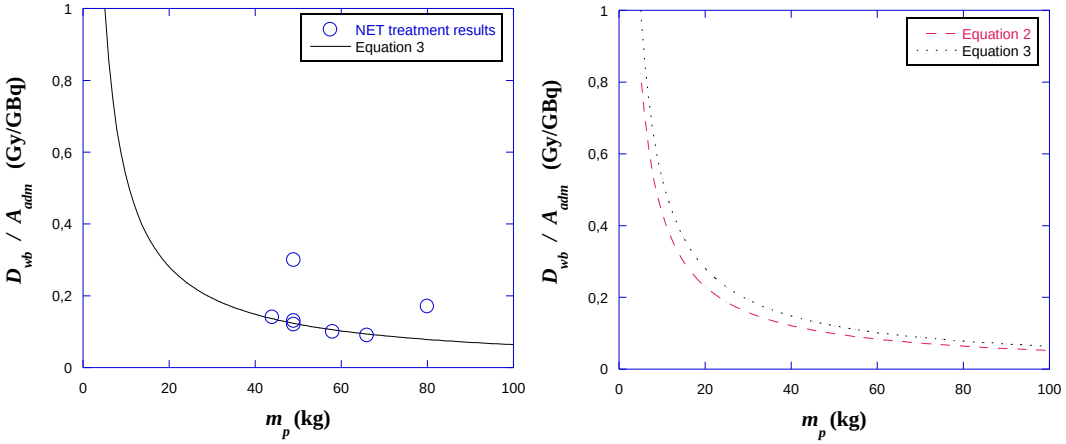


Figure 4. Results for $D_{wb}/A_{adm}$ as a function of $m_p$ in NET patients (left), and (right) comparison of Eqs. (2) and (3), representing $D_{wb}/A_{adm}$ as a function of $m_p$ for NB and NET patients, respectively.

## 4. DISCUSSION

In NB and NET treatments with $^{131}$I-mIBG, very different schedules have been reported[13-19], often using prescriptions in terms of a fixed activity or a predetermined activity per body mass. For treatment of NB, the most widely used dose scheduling approach is that of Gaze *et al.*[17] and is based on planning of $D_{wb}$ using two treatment fractions. In NET treatments, such established schedules are still lacking, although a similar approach could be adopted to tailor $D_{wb}$ with regard to the risk of inducing hematologic and non-hematologic toxicities.

The analysis of patient data by Eqs. (2) and (3) for NB and NET treatments, respectively, was motivated by a practical need for activity prescriptions in situations when $\tau_{wb}$ for an individual patient has not yet been measured, such as for the first activity administration in a dosimetry-based schedule. Eqs. (2) and (3) should be thus regarded as an alternative to prescribing a fixed activity or activity per body mass. For comparison with the schedule given by Gaze *et al.*[17], Eq. (2) was reformulated in terms of $D_{wb}$ as a function of $A_{adm}/m_p$ (Figure 5). Eq. (2) has the advantage of taking the decreasing values of $S_{wb\leftarrow wb}$ into account, which implies that for the heavier patients, a lower activity can be administered. For instance, for a 70 kg patient the activity to administer is decreased by approximately 12% as compared to using 444 MBq/kg[17]. Comparison was also made to the work by Matthay *et al.*[22], where a linearly increasing $D_{wb}$ was obtained when presented as a function of $A_{adm}/m_p$, with a considerably larger variability in $D_{wb}$ for higher values of $A_{adm}/m_p$. Their results thus agree with Eq. (2), both concerning the linear increase and the larger variability in $D_{wb}$ for higher values of $A_{adm}/m_p$. Due to the limited amount of data for NET patients (Figure 4), Eq. (3) should be treated with caution and regarded as preliminary. Comparison studies with results from other centers would be desirable, especially for $m_p$ values outside the included range. However, in the literature, reported dosimetry values for $^{131}$I-mIBG treatment of NET patients are still few. In this study, $D_{wb}/A_{adm}$ values are higher and show a wider range for NB than for NET

treatments consistent with those reported in Sudbrock *et al.*[9] and Hindorf *et al.*[27]. Figures 3 and 4, based on Eqs. (2) and (3), respectively, provide an explanation for those results based on the dependence of $D_{wb}/A_{adm}$ on $m_p$. It is important to note that Eqs. (2) and (3) are not intended as replacement for dosimetry-based schedules, since $\tau_{wb}$ of individual patients may vary to a high degree. For instance, in $T_{NB}2$, the patient ($m_p$=13kg) suffered from a nephropathy and the obtained $D_{wb}/A_{adm}$ value was lower that the value obtained by Eq. (2), as seen in Figure 3 and Table 3. In $T_{NET}4$ and $T_{NET}5$ ($m_p$=49 kg and 80 kg, respectively), patients had an extensive tumor burden and their $D_{wb}/A_{adm}$ values were notably higher than the value obtained from Eq. (3), as seen in Figure 4 (left) and Table 5. Thus, whole-body dosimetry measurements during the first administration would still be necessary in order to calculate the activity to deliver in the second administration.

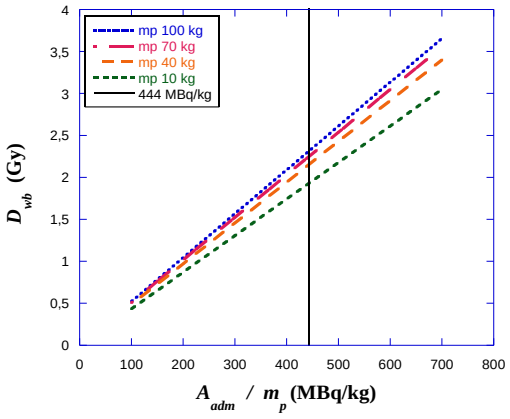


Figure 5. Representation of Eq. (2) in terms of $D_{wb}$ as a function of $A_{adm}/m_p$. The vertical line represents the activity of 444MBq/kg given in the schedule by Gaze *et al.*[17].

$D_{wb}$ is generally used as a surrogate for $D_{rm}$ in $^{131}$I-mIBG therapy. In this study, values of $D_{rm}$ were found to be between 60% and 70% of $D_{wb}$, which is reasonable considering the modest contribution of the self-absorbed dose and the values for the $S_{wb\leftarrow wb}/S_{rm\leftarrow wb}$ ratio. In patients in whom there is red-marrow and/or bone uptake, it is generally recommended to use imaging-based estimates of $D_{rm}$[26,36,37], as blood-based values may underestimate the real value. However, results from the blood-based method may be a good approximation when red-

marrow or bone uptake is localized to small regions[36]. For the patients in this study where red-marrow dosimetry was performed, in five patients ($T_{NB}9a$, $T_{NB}9b$, $T_{NET}2$, $T_{NET}6a$ and $T_{NET}6b$) uptake in red marrow or bone was seen in separate SPECT-CT studies, but involved less than 5% of the total marrow volume, thus justifying the use of the blood-based dosimetry method.

A further analysis was performed by comparison to the results from Matthay *et al.*[22], who studied dose escalation of $^{131}$I-mIBG in treatment of NB with autologous stem-cell rescue. In their work, none of the 18 patients who were given activities < 555 MBq/kg required stem cell infusion, whereas two of seven patients given 555 MBq/kg and nine of 17 patients given 666 MBq/kg required stem-cell support. Using Eq. (2) and the obtained mean value of $D_{wb}/D_{rm}$ for NB of 1.5, an estimation of $D_{rm}$ for values of $A_{adm}/m_p$ of 444, 555 and 666 MBq/kg was made (Figure 6). Activities of 666 MBq/kg resulted in a $D_{rm}$ which for most $m_p$ exceeded the tolerance dose of approximately 1.6—2 Gy[25]. Giving 555 MBq/kg, $D_{rm}$ close to 2 Gy were obtained, whereas for 444 MBq/kg, $D_{rm}$ were well below 2 Gy. Figure 6 also shows the $D_{wb}$ as estimated from Eq. (2), indicating that on average 444 MBq/kg[17] results in $D_{wb}$ above 2 Gy for patients above approximately 15 kg.

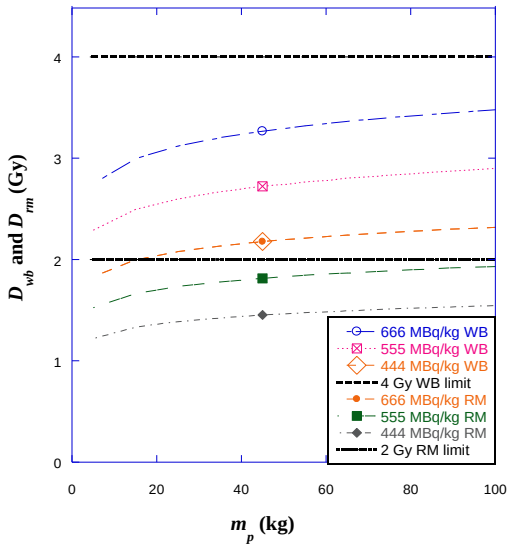


Figure 6. Representation of $D_{wb}$ and $D_{rm}$ as function of $m_p$ for NB patients, for $A_{adm}$ of 444, 555 and 666 MBq/kg. Values have been derived from Eq. (2) and a value of $D_{wb}/D_{rm}$ of 1.5.

The grade of hematologic toxicity (Table 7) shows that caution must be exercised for high-activity treatments. Unlike that of Buckley *et al.*[25], this study found no correlation between the grade of hematologic toxicity and $D_{wb}$. Notably, in $T_{NET}3$, a $D_{wb}$ of 1.3 Gy was delivered but the patient suffered grade-4 toxicity (platelets, leukocytes and neutrophils) and in $T_{NET}4$, the patient with multiple bone metastases received a $D_{wb}$ of 4.1 Gy but did not exceed grade-3 toxicity. As with $D_{wb}$, no correlation was found between the grade of hematologic toxicity and $D_{rm}$. There are several possible reasons for the lack of correlation found between $D_{rm}$ and $D_{wb}$ with hematologic toxicity. Among those are the low number of patients included, the different ages of patients, the diversity of NETs (pheochromocytoma, carcinoid tumor and paraganglioma), prior hematotoxic treatments, and the way the cross-absorbed dose to the red marrow is calculated in Eq. (B1). Regarding the latter point, if the activity in the remainder of the body is mainly localized in tumors, then its contribution to $D_{rm}$ is likely to be heterogeneous with an important proportion of the red marrow receiving absorbed doses below tolerance values. In a study of hematological toxicity in EBRT performed by Petersson *et al.*[38], it was shown that the severity of toxicity correlated with the volume fraction of red marrow that was irradiated. In this study the volume distribution of $D_{rm}$ was not addressed, and so, depending on the tumor burden, two treatments with the same value of $D_{rm}$ obtained from Eq. (B1) may show different hematologic toxicity. These results indicate the need to improve currently used methods for red-marrow dosimetry in MRT, taking the heterogeneous distribution of internal absorbed doses into account.

## 5. CONCLUSIONS

In treatments with $^{131}$I-mIBG, the activity to administer in order to give a prescribed $D_{wb}$ varies from patient to patient. In this study, consistent values of $D_{wb}/A_{adm}$ were obtained when

400 determined for different administrations in the same patient, whereas a considerable variation was seen among patients. These results thus support the use of absorbed-dose planning for multiple-fraction treatment. Moreover, an expression was proposed for prescription of the activity for the first administration, which takes into account the dependence of $D_{wb}/A_{adm}$ on $m_p$, to be used at the stage when dosimetric data for the individual patient have not yet been 405 measured. For red marrow, $D_{rm}$ was found to be between 60% and 70% of $D_{wb}$.

**Competing interests**

The authors declare that they have no competing interests.

## APPENDIX A: WHOLE-BODY ABSORBED DOSE ($D_{wb}$)

410 $D_{wb}$ is given by:

$$D_{wb} = \tilde{A}_{wb} S_{wb \leftarrow wb} = A_{adm}\, \tau_{wb}\, S_{wb \leftarrow wb} \qquad \text{(A1)}$$

where $\tilde{A}_{wb}$ is the cumulated activity in the whole body ($wb$) and $S_{wb \leftarrow wb}$ is the whole-body absorbed dose per cumulated activity in $wb$, calculated according to Cristy *et al.*[39]:

$$S_{wb \leftarrow wb} = 1.34 \times 10^{-4}\, m_p^{-0.921} \qquad \text{(A2)}$$

in Gy MBq$^{-1}$ h$^{-1}$, and $m_p$ is the patient mass (kg). The residence time $\tau_{wb}$ is determined from the values $r(t)$ obtained from measurement (Eq. (1)), by fitting one exponential function for 415 each of the $n$ components and performing integration, according to:

$$\tau_{wb} = \sum_{i=1}^{n} \frac{a_i - a_{i+1}}{\lambda_i} \qquad \text{(A3)}$$

where coefficient $a_i$ is the initial value for component $i$ and $\lambda_i$ is the effective half-life, in unit h$^{-1}$, for the respective component[25]. The value of $n$ was set to 3 and 2, for dose-rate measurements and gamma-camera imaging, respectively.

420

## APPENDIX B: RED-MARROW ABSORBED DOSE ($D_{rm}$)

$D_{rm}$ is given by:

$$D_{rm} = \tilde{A}_{rm} S_{rm \leftarrow rm} + \tilde{A}_{rb} S_{rm \leftarrow rb} \quad \text{(B1)}$$

where $\tilde{A}_{rm}$ and $\tilde{A}_{rb} = \tilde{A}_{wb} - \tilde{A}_{rm}$ are the cumulated activities in the red marrow (*rm*) and the remainder of the body (*rb*), respectively, $S_{rm \leftarrow rm}$ is the factor describing the self-absorbed dose from activity residing in *rm*, and $S_{rm \leftarrow rb}$ is the factor describing the cross-absorbed dose from activity residing in *rb* and is given by the expression:

$$S_{rm \leftarrow rb} = S_{rm \leftarrow wb} \frac{m_{wb}}{m_{rb}} - S_{rm \leftarrow rm} \frac{m_{rm}}{m_{rb}} \quad \text{(B2)}$$

where $S_{rm \leftarrow wb}$ is the factor describing the cross-absorbed dose from activity residing in *wb*, and $m_{wb}$, $m_{rb}$ , and $m_{rm}$, are the masses of *wb*, *rb* and *rm*, respectively. *S*-values and values of $m_{wb}$, $m_{rb}$ and $m_{rm}$ were obtained for the male and female reference phantoms in OLINDA/EXM[40], and were scaled to the mass of the individual patient.

$\tilde{A}_{rm}$ was obtained following:

$$\tilde{A}_{rm} = [\tilde{A}]_{blood} \, RMBLR \cdot m_{rm} \quad \text{(B3)}$$

where $[\tilde{A}]_{blood}$ is the cumulated activity in blood per unit of volume, and *RMBLR* is the red marrow-to-blood activity concentration ratio, which was set to 1[41,42].

## APPENDIX C: ESTIMATION OF UNCERTAINTIES

The standard deviation in $D_{wb}$ was determined by uncertainty propagation through Eq. (A1), considering only the uncertainty in $\tilde{A}_{wb}$ as determined from standard deviations of $A_{adm}$ and $\tau_{wb}$. The relative standard deviation of $A_{adm}$ was estimated to be 5%. The uncertainty in $\tau_{wb}$ (Eq. (A3)) depended on the uncertainty in the parameters $a_i$ and $\lambda_i$, which in turn depended on the uncertainty of $r(t)$ in Eq. (1), and the number of data points used for curve fitting. The standard deviation in $r(t)$, $\sigma_r$, was calculated by uncertainty propagation through the expression for $r(t)$. For dose rate measurements, uncertainties in $R_A(t)$ and $R_P(t)$ were primarily related to measurements of patient-detector distance and fluctuations in the measured value, for which the relative standard deviations were estimated to be 5% in both cases. For gamma camera measurements, the major sources of uncertainty in $R_A(t)$ and $R_P(t)$ were assumed to be operator dependency in delineation of the whole-body ROI, and a variability in the accuracy of Eq. (1) due to different attenuation and scatter conditions for different times after administration. The relative standard deviations of these effects were estimated to be 7% and 10%, respectively. The uncertainty contribution to $\tau_{wb}$ from curve fitting was determined from simulated, typical time-retention curves, consisting of three components. This simulation was performed by generating time-series of values $r(t)$ using an analytical expression, and then replacing each data point with a value which was sampled from a normal distribution with standard deviation $\sigma_r$. One hundred simulations were performed, giving a relative standard deviation for $\tau_{wb}$ of approximately 19% for both measurement techniques. The relative standard deviations in $\tilde{A}_{wb}$ and thus in $D_{wb}$, were approximately 20%. Because the main contribution to $D_{rm}$ was the cross-absorbed dose, the uncertainty in $D_{rm}$ was estimated to be approximately equal to the uncertainty in $D_{wb}$.

[a] Author to whom correspondence should be addressed. Electronic mail: pablo.minguezgabina@osakidetza.net. Telephone: +34 94 600 61 73

[1]J. A. O'Neill, P. Littman, P. Blitzer, K. Soper , J. Chatten and H. Shimada. "The role of surgery in localized neuroblastoma." J. Pediatr. Surg. **20**, 708-712 (1985).

[2]G. Akerström and P. Hellman. "Surgery on neuroendocrine tumors." Best. Pract. Res. Clin. Endocrinol. Metab. **21**, 87-109 (2007)

[3]J. C. Sisson and G. A. Yanik. "Theranostics: Evolution of the Radiopharmaceutical Meta-Iodobenzylguanidine in Endocrine Tumors." Semin. Nucl. Med. **42**, 171-184 (2012)

[4]F. Giammarile, A. Chiti, M. Lassmann, B. Brans and G. Flux. "EANM procedure guidelines for $^{131}$I-meta-iodobenzylguanidine (131I-mIBG) therapy." Eur. J. Nucl. Med. Mol. Imaging. **35,** 1039–1047 (2008)

[5]K. C. Loh, P. A. Fitzgerald, K. K. Matthay, P. P. Yeo and D. C. Price ."The treatment of malignant pheochromocytoma with iodine-131 metaiodobenzylguanidine (131I-MIBG): a comprehensive review of 116 reported patients." J. Endocrinol. Invest. **20(11)**, 648-658 (1997)

[6]E. M. Prvulovich, R. C. Stein, J. B. Bomanji, J. A. Ledermann, I. Taylor and P. J. Ell. "Iodine-131-MIBG Therapy of a Patient with Carcinoid Liver Metastases." J. NucI. Med. **39**, 1743-1745 (1998)

[7]S. G. DuBois and K. K. Matthay." Radiolabeled meaiodobenzylguanidine for the treatment of neuroblastoma." Nucl. Med. Bio. **35**, 35-48 (2008)

[8]G. Gnanasegaran, N. Kapse and J. R. Buscombe. "Recent Trends in Radionuclide Imaging and Targeted Radionuclide Therapy of Neuroendocrine Tumors." Indian J. Nucl. Med. **20**, 55-66 (2005)

[9]F. Sudbrock, M. Schmidt, T. Simon, W. Eschner, F. Berthold and H. Schicha. "Dosimetry for $^{131}$I-MIBG therapies in metastatic neuroblastoma, phaeochromocytoma and paraganglioma." Eur. J. Nucl. Med. Mol Imaging. **37**, 1279–1290 (2010)

[10]M. N. Gaze and N. L. Fersht. "Current experience with mIBG therapy in combination with chemotherapy and radiosensitizers." Nucl. Med. Biol. **35**, 21-26 (2008)

[11]J. Toporski, M. Garkavij, J. Tennvall, I. Ora, K. Sjögreen Gleisner, J. H. Dykes, S. Lenhoff, G. Juliusson, S. Scheding, D. Turkiewicz and A. N. Bekassy. "High-Dose Iodine-131-Metaiodobenzylguanadine with Haploidentical Stem Cell Transplantation and Posttransplant Inmunotherapy in Children with Relapsed/Refractory Neuroblastoma." Biol. Blood Marrow Transplant **15**,1077-1085 (2009)

[12]C. Chiesa, R. Castellani, M. Mira, A. Lorenzoni and G. D. Flux. "Dosimetry in 131I-MIBG therapy: moving toward personalized medicine." Q. J. Nucl. Med. Mol. Imaging **57**,161-170 (2013)

[13]G. K. Gedik, C. A. Hoefnagel, E. Bais and R. A. Valdes Olmos. "$^{131}$I-mIBG therapy in metastatic phaeochromocytoma and paraganglioma." Eur. J. Nucl. Med. Mol. Imaging **35**, 725–733 (2008)

[14]S. D. Safford, R. E. Coleman, J. P. Gockerman, J. Moore, J. M. Feldman, G. S. Leight, D. S. Tyler and J. Olson. "Iodine -131 metaiodobenzylguanidine is an effective treatment for malignant pheochromocytoma and paraganglioma." Surgery **134 (6)**,956-962 (2003)

[15]T. I. Kang, P. Brophy, M. Hickeson, S. Heyman, A. E. Evans, M. Charron and J. M. Maris. "Targeted radiotherapy with submyeloablative doses of 131I-MIBG is effective for disease palliation in highly refractory neuroblastoma." J. Pediatr. Hematol. Oncol. **25(10)**,769-773 (2003)

[16]K. K. Matthay, A. Quach, J. Huberty, B. L. Franc, R. A. Hawkins, H. Jackson, S. Groshen, S. Shusterman, G. Yanik, J. Veatch, P. Brophy and J. G. Villablanca. "Iodine-131-metaiodobenzylguanidine double infusion with autologous stem-cell rescue for neuroblastoma: a new approaches to neuroblastoma therapy phase I study." J. Clin. Oncol. **27(7)**, 1020-1025 (2009)

[17]M. N. Gaze, Y. Chang, G. D. Flux, R. J. Mairs, F. H. Saran and S. T. Meller. « Feasibility of dosimetry-based high-dose 131I-meta-iodobenzylguanidine with topotecan as a radiosensitizer in children with metastatic neuroblastoma." Cancer Biother. Radiopharm. **20,** 195–199 (2005)

[18]B. Rose, K. K. Matthay, D. Price, J. Huberty, B. Klencke, J. A. Norton and P. A. Fitzgerald. "High-dose 131I-Metaiodobenzylguanidine therapy for 12 patients with malignant pheocromocytoma." Cancer **98(2)**, 239-248 (2003)

[19]K. K. Matthay, J. P. Huberty, R. S. Hattner, A. R. Ablin, B. L. Engelstad, S. Zoger, B. H. Hasegawa and D. Price. "Efficacy and safety of [131I]metaiodobenzylguanidine therapy for patients with refractory neuroblastoma." J. Nucl. Biol. Med. **35**,244-247 (1991)

[20]M. R. Castellani, S. Seghezzi, C. Chiesa, G. L. Aliberti, M. Maccauro, E. Seregni, E. Orunesu, R. Luksch and E. Bombardieri. "(131)I-MIBG treatment of pheochromocytoma: low versus intermediate activity regimens of therapy." Q. J. Nucl. Med. Mol. Imaging **54(1)**, 100-113 (2010)

[21]S. Gonias, R. Goldsby, K. K. Matthay, R. Hawkins, D. Price, J. Huberty, L. Damon, C. Linker, A. Sznewajs, S. Shiboski and P. Fitzgerald. "Phase II Study of High-Dose [131I]Metaiodobenzylguanidine Therapy for Patients With Metastatic Pheochromocytoma and Paraganglioma." J. Clin. Oncol. **27**,4162-4168 (2009)

[22]G. D. Flux, S. J. Chittenden, F. Saran and M. N.Gaze. "Clinical applications of dosimetry for mIBG therapy." Q. J. Nucl. Med. Mol. Imaging. **55**, 116-125 (2011)

[23]S. G. DuBois, J. Messina, J. M. Maris, J. Huberty, D. V. Glidden, J. Veatch, M. Charron, R. Hawkins and K. K. Matthay. "Hematologic Toxicity of High-Dose Iodine-131–Metaiodobenzylguanidine Therapy for Advanced Neuroblastoma." J. Clin. Oncol. **22**, 2452-2460 (2004)

[24]G. Bleeker, R. A. Schoot, H. N. Caron, J. de Kraker, C. A. Hoefnagel, B. L. van Eck and G. A. Tytgat. "Toxicity of upfront $^{131}$I-metaiodobenzylguanidine ($^{131}$I-MIBG) therapy in newly

565 diagnosed neuroblastoma patients: a retrospective analysis." Eur. J. Nucl. Med. Mol. Imaging **40**, 1711-1717 (2013)

[25]S. E. Buckley, S. J. Chittenden, F. H. Saran, S. T. Meller and G. D. Flux. "Whole-Body Dosimetry for Individualized Treatment Planning of $^{131}$I-mIBG Radionuclide Therapy for
570 Neuroblastoma." J. Nucl. Med. **50**, 1518-1524 (2009)

[26]K. K. Matthay, C. Panina, J. Huberty, D. Price, D. V. Glidden, H. R. Tang, R. A. Hawkins, J. Veatch and B. Hasegawa. "Correlation of tumor and whole-body dosimetry with tumor response and toxicity in refractory neuroblastoma treated with $^{131}$I-mIBG." J. Nucl. Med. **42**,
575 1713–1721 (2001)

[27]C. Hindorf, G. Glatting, C. Chiesa, O. Linden and G. Flux. "EANM Dosimetry Committee guidelines for bone marrow and whole-body dosimetry." Eur. J. Nucl. Med. Mol. Imaging **37,** 1238–1250 (2010)

580

[28]M. Lassmann, C. Chiesa, G. Flux and M. Bardies. "EANM Dosimetry Committee guidance document: good practice of clinical dosimetry reporting." Eur. J. Nucl. Med. Mol. Imaging **38**, 192-200 (2011)

585 [29]International Atomic Energy Agency, "Release of patients after radionuclide therapy," Safety Report Series No. 63, IAEA, Vienna (2009)

[30]R. Loevinger, T. Budinger and E. Watson. "MIRD primer for absorbed dose calculations." Society of Nuclear Medicine; New York (1988)

[31]A. C. Traino, M. Ferrari, M. Cremonesi and M. G. Stabin. "Influence of whole-body mass on the scaling of S-factors for patient-specific, blood-based red marrow dosimetry." Phys. Med. Biol. **52**, 5231–5248 (2007)

[32]G. D. Flux, M. J. Guy, R. Beddows, M. Pryor and M. A. Flower. "Estimation and implications of random errors in whole-body dosimetry for targeted radionuclide therapy." Phys. Med. Biol. **47**, 3211–3223 (2002)

[33]M. G. Stabin. "Uncertainties in internal dose calculations for radiopharmaceuticals." J. Nucl. Med. **49**, 853-860 (2008)

[34]K. Norrgren, S. L. Svegborn, J. Areberg and S. Mattsson. "Accuracy of the Quantification of Organ Activity from Planar Gamma Camera Images." Cancer Biother. Radiopharm. **18**,125-131 (2003)

[35]A. Trotti, A. D. Colevas, A. Setser, V. Rusch, D. Jacques, V. Budach, C. Langer, B. Murphy, R. Cumberlin, C. N. Coleman and P. Rubin. "CTCAE v3.0: development of a comprehensive grading system for adverse effects of cancer treatment." Semin. Radiat. Oncol **13,** 176–181 (2003)

[36]J. A. Siegel. "Establishing a Clinically Meaningful Predictive Model of Hematologic Toxicity in Nonmyeloablative Targeted Radiotherapy: Practical Aspects and Limitations of Red Marrow Dosimetry." Cancer Biother. Radiopharm. **20**,126-140 (2005)

[37]C. Hindorf, O. Linden, J. Tennvall, K. Wingärdh and S. E. Strand. "Time dependence of the activity concentration ratio of red marrow to blood and implications for red marrow dosimetry." Cancer. **94**, 1235-1239 (2002)

[38]K. Petersson, M. Gebre-Medhin, C. Ceberg, P. Nilsson, P. Engström, T. Knöös and E. Kjellén. "Haematological toxicity in adult patients receiving craniospinal irradiation. Indication of a dose-bath effect." Radiother. Oncol. http://dx.doi.org/10.1016/j.radonc.2014.01.020. (2014).

[39]M. Cristy and K. Eckerman."Specific Absorbed Administrations of Energy at Various Ages from Internal Photon Sources." ORNL/TM-8381 V1-V7. Oak Ridge, TN: Oak Ridge National Laboratory (1987)

[40]M. G. Stabin, R. B. Sparks and E. Crowe. "OLINDA/EXM: the second-generation personal computer software for internal dose assessment in nuclear medicine." J. Nucl. Med. **46**, 1023-1027 (2005)

[41]G. Sgouros. "Bone marrow dosimetry for radioimmunotherapy: theoretical considerations." J. Nucl. Med. **34**, 689-694 (1993)

[42]F. Forrer, E. P. Krenning, P.P. Kooij, B. F. Bernard, M. Konijnenberg, W. H. Bakker, J. J. M. Teunissem, M. de Jong, K. van Lom and W. W. de Herder. "Bone marrow dosimetry in peptide receptor radionuclide therapy with [$^{177}$Lu-DOTA0,Tyr$^{3}$] octreotate." Eur. J. Nucl.. Med. Mol. Imaging **36**, 1138-1146 (2009)